ACADEMIC PRESS

Available online at www.sciencedirect.com
SCIENCE DIRECT®

Journal of Catalysis 213 (2003) 241–250

JOURNAL OF CATALYSIS

www.elsevier.com/locate/jcat

Mechanism of selective catalytic reduction of NO in the presence of excess O_2 over Pt/Si-MCM-41 catalyst

S.-C. Shen and S. Kawi *

Department of Chemical and Environmental Engineering, National University of Singapore, Singapore 119260

Received 24 June 2002; revised 9 September 2002; accepted 30 September 2002

Abstract

The reaction mechanism for the selective catalytic reduction (SCR) of nitric oxide (NO) over Pt/Si-MCM-41 catalyst has been studied by XPS and in-situ Fourier transform infrared (FTIR) spectroscopies as well as TPR. The XPS results indicate that Pt species are reduced during the reaction of NO-SCR in the presence of excess oxygen. The reduced Pt species are found not to be completely oxidised after they have been in contact with NO or O_2 at the reaction temperature. FTIR results indicate that CO is one of the reaction intermediates taking part in the selective reduction of NO. The possible reaction mechanism for the selective catalytic reduction of NO over Pt/Si-MCM-41 catalyst is proposed.

Keywords: De-NO_x; SCR; Pt/Si-MCM-41; Mechanism; XPS; In-situ FTIR; TPR

1. Introduction

Diesel or lean-burn engines are faced with the serious problems of reducing harmful pollutant of a few hundred parts per million (ppm) of NO_x (nitric oxide NO plus nitrogen dioxide NO_2) in a large quantity of oxygen (several percent) with traces of hydrocarbons. Moreover, NO does not spontaneously decompose or react with hydrocarbons in the absence of a catalyst. Thus, the questions need to be solved are: How could a catalyst reduce such traces of NO_x catalytically under an oxidative atmosphere with the help of traces of hydrocarbons? How is a nitrogen (N_2) molecule formed from two separated NO molecules? To answer these questions, it is necessary for us to study the reaction's mechanisms and to gather the necessary information of all the parameters involved in such reactions.

Concerning the reaction mechanism over metal exchanged zeolites, there is one general mechanistic route which has been proposed by several authors [1–6]. According to this mechanism, which may be called nitric oxide oxidation mechanism, nitric oxide is first catalytically oxidised to nitrogen dioxide, which then reacts with the hydrocarbon to yield nitrogen-containing organic compounds, and a further reaction of this compound finally leads to the formation of nitrogen. The details of this reaction sequence are, however, discussed controversially. The formation of organic nitro, nitroso or nitrite compounds in the initial reaction between NO_2 and the hydrocarbon is plausible and has been proposed by several authors [7–10]. Furthermore, nitrile and/or isocyanate species, possibly derived from the nitro or nitroso compounds, have been reported to form during the reaction [11–13]. Several authors have proposed that these species can react with O_2 [7,9,11], NO [3,7,12], or NO_2 [13,14] to form nitrogen. Cowan et al. [8] have shown that isocyanic acid can be hydrolysed by water present in the reaction system to form ammonia, which is a compound well-known to be efficient in reducing nitrogen oxides to nitrogen. Takeda and Iwamoto [14] also speculated that in the presence of water, isocyanic acid might be hydrolysed to ammonia and carbon dioxide. Using infrared spectroscopy, Poignant et al. [15] found an evidence for the formation of ammonia during the reduction of nitric oxide by propane in the presence of oxygen.

Supported platinum-based catalysts were found to have high activity at low temperature [16–22] and not to be significantly affected by the presence of water in the exhaust stream [23]. However, these catalysts have some limitations for practical application as they have narrow operation temperature and tend to form nitrous oxide [21–24]. Despite

* Corresponding author.
E-mail address: chekawis@nus.edu.sg (S. Kawi).

0021-9517/02/$ – see front matter
PII: S0021-9517(02)00048-9

this, more attention has focused recently on the performance of a platinum-based catalyst for its potential commercial application for SCR of NO_x from cold-start vehicle. Although the reaction mechanism on a Pt-based catalyst has been investigated [25–35], there is still a limited understanding on the fundamental role of Pt species and its surface chemistry involved in the de-NO_x reaction.

For the selective catalytic reduction of NO with hydrocarbon over a Pt-based catalyst, it has been suggested that the activation of hydrocarbon occurs first to form the partially oxidised intermediates of hydrocarbon ($C_xO_yH_z$), which then react with NO or NO_2 to form N_2 on the same type of active sites [36]. On the other hand, Burch et al. [37] suggested that the SCR of NO occurred simultaneously on these two reaction paths. In these two reaction paths, the main route is that NO dissociates on the reduced Pt active sites. N_2 and N_2O are formed by combination of adsorbed N with N or NO, respectively. Oxygen from NO is retained on the surface of the Pt and blocks the surface for further adsorption and dissociation of NO. The reductant is then responsible for the removal of surface oxygen and regeneration of the Pt sites to be in reduced state. The minor mechanism involves carbon-assisted decomposition of NO at the reduced Pt site adjacent to adsorbed carbon-containing intermediates.

It has also been found that different platinum precursor and catalyst supports have remarkable effects on the activity of the resulting catalyst for NO reduction [37,38]. Long and Yang [39] reported that Pt/MCM-41 provided highest specific reaction rate for selective catalytic reduction of NO as compared with Pt supported on other conventional catalyst supports. The new type of mesoporous catalyst attracts great interests to the application in SCR of NO_x and its catalytic performance has been widely studied [40–45]. The state of Pt and reaction intermediates on Pt/MCM-41 catalyst during NO reduction reaction have been studied by some researchers. The change in the oxidation state of Pt over MCM-41 during DeNO_x reaction has been investigated by in-situ XANES [46,47]. The oxidation/reduction of Pt/MCM-41 was found not to be influenced by the presence of water vapour. However, the oxidation state of Pt species was strongly dependent on the nature of mesoporous supports (SiO_2 or Al_2O_3) and reductants (C_3H_8 or C_3H_6). Schießer et al. [48] studied the surface species during HC-SCR of NO over Pt supported on mesoporous Al_2O_3 catalyst and a reaction pathway was concluded. Nevertheless, the overall reaction mechanism for HC-SCR of NO over Pt-based catalyst has not been fully explored. It is of interest to investigate the reaction mechanism of HC-SCR of NO over Pt supported over siliceous MCM-41 materials as the surface reaction can be influenced by the surface chemical properties of support and this reaction mechanism over Pt/Si-MCM-41 catalyst still has not been studied in detail.

The objective of this work is to study the fundamental aspects of lean NO reduction reaction over Pt supported on novel mesoporous MCM-41 material. This study aims to utilize XPS and in-situ FTIR spectroscopies toward the understanding of the formation of these active sites on the catalyst and their involvement in the reaction mechanism of NO-SCR. A fundamental understanding of the reaction mechanism of NO-SCR is believed to be essential for the development of a catalyst and improvement for potential application.

2. Experimental

Si-MCM-41 mesoporous material was prepared as follows. Silicate gel was prepared by adding 6 g of silica aerosol to NaOH solution (prepared by dissolving 2 g of NaOH in 90 g of de-ionized water) under stirring and heating until all aerosol was completely dissolved. A solution of CTMABr (cetyltrimethylammonium bromide), which was prepared by dissolving 9.1 g of CTMABr in 50 g of de-ionized water, was added dropwise to the silicate gel under stirring at 25 °C. The pH value of the gel mixture was adjusted to 11.5 using 2 N of HCl solution. After stirring continuously for additional 6 h at 25 °C, the gel mixture was transferred into a polypropylene bottle and statically heated at 100 °C for 72 h. The resulting solid product was recovered by filtration, washed with de-ionized water, and dried at 50 °C for 24 h. The solids were calcined in air at 600 °C for 10 h, using a heating rate of 1 °C/min.

Pt/Si-MCM-41 was prepared by incipient wetness impregnation of MCM-41 mesoporous support with an aqueous solution of tetraamineplatinum(II) nitrate (Aldrich). The amount of solution was designed in such a way that the amount of liquid was just enough to fill up the pores of the support. Following the impregnation, the sample was dried at 100 °C for 8 h and then calcined in air at 500 °C for 3 h.

Pt/Al_2O_3 catalyst was prepared by impregnation of commercial Al_2O_3 (Strem) with tetraamineplatinum(II) nitrate aqueous solution, following the same preparation procedure of Pt/Si-MCM-41. SiO_2 support was obtained from direct drying of silica gel solution (Ludox, Dupont), then followed by calcination at 500 °C. Pt/SiO_2 catalyst was prepared using the same preparation method of Pt/Al_2O_3 catalyst.

The catalytic activities of the Pt/Si-MCM-41 catalysts were evaluated by using a micro-catalytic reactor (OD 1/4 inch) in a steady-state plug flow mode. The total gas flow rate was 200 ml/min and 0.45 g catalyst was packed in the reactor. The reaction mixture typically consisted of 1000 ppm of NO, 1000 ppm of C_3H_6 or C_3H_8, and 5 vol.% of O_2 (balanced in He). The concentration of HC, CO_2, N_2O, and H_2O in the reaction exhaust was analyzed by a gas chromatograph (Shimadzu GC-17A) equipped with Porapak Q Column, and that of NO_x and O_2 was recorded by a chemiluminescence NO_x/O_2 analyzer (Shimadzu NOA-7000).

Temperature programmed reduction (TPR) analysis was carried out by flowing 40 ml/min of H_2 (5 vol.%)/N_2 and raising the catalyst temperature from room temperature to

650 °C at 5 °C/min. The change in hydrogen concentration was measured by a gas chromatograph (Shimadzu GC-8A) equipped with a thermal conductivity detector. The water produced during the reduction was trapped in a 5A molecular sieve column.

The oxidation states of surface platinum species on MCM-41 was characterized by X-ray photoelectron spectroscopy (XPS) using a Kratos AXIS analytical instrument. An Mg-K_α X-ray source ($h\nu = 1253.6$ eV) with an analyzer pass energy of 80 eV was operated at 10 mA and 15 kV. The pressure in the XPS analysis chamber was less than 10^{-9} Torr.

The powder X-ray diffraction patterns of samples were recorded using a SHIMADZU XRD-6000 powder diffractometer, where Cu-K_α ray was used as the X-ray source. The surface areas and pore properties of Pt/MCM-41 materials were analyzed by nitrogen physisorption at 77 K using a Quantachrome Auto-Sorb1 Analyzer.

Infrared spectra were collected using a SHIMADZU FTIR-8700 Fourier transform infrared spectrometer. 15 mg of catalyst sample was pressed (at a pressure of 4 ton/cm^2 for 30 min) into a self-supported wafer (16 mm in diameter). Transmission spectra were collected in the single beam mode with a resolution of 2 cm^{-1} after treatment under different conditions. Reference spectra of the clean surface in flowing He were collected separately and the difference of the spectra between the samples and the corresponding reference were obtained. A quartz IR cell with CaF_2 windows cooled by flowing water was used. A heating wire, which was wrapped around the quartz insulator near the sample wafer, allowed collection of in-situ spectra at 150–350 °C. The temperature was monitored through a thermocouple located in the cell and in close proximity with the catalyst sample. Certified gas mixtures consisting of 2500 ppm of NO in He (Soxal), 25% of O_2 in He (Soxal), 2500 ppm of C_3H_6 in He, and a 99.999% He carrier gas (Messer) were used to prepare the different gas mixtures. A typical concentration used in this study was 1000 ppm of NO, 1000 ppm of C_3H_6, and 5.0% of O_2. Gases were mixed at appropriate amounts and introduced to the IR quartz cell using a system of needle valves and mass flow meters. The volumetric flow rate of the gas mixtures was held at 50 ml/min.

3. Results and discussion

3.1. XPS study

The mesoporous structure of Pt/Si-MCM-41 materials is characterized by XRD and N_2 adsorption. Figure 1 displays the XRD patterns of 1wt.% Pt/Si-MCM-41 catalyst before and after reaction in NO–C_3H_6–O_2 system at temperatures of 200 to 500 °C. An intensive peak observed at $2\theta = 2.44°$ for both samples corresponds to the (100) diffraction of the mesoporous MCM-41 framework. The specific surface area of 1wt.% Pt/Si-MCM-41 catalyst is ~ 1000 m^2/g. A narrow

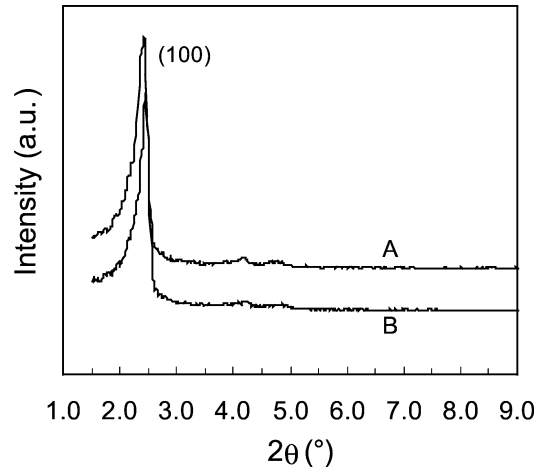

Fig. 1. XRD patterns of 1wt.% Pt/Si-MCM-41 catalyst before (A) and after (B) reaction in NO–C_3H_6–O_2 system.

pore size distribution peak ($\sim$ 26 Å) is observed for Pt/Si-MCM-41 catalyst before and after reaction in NO–C_3H_6–O_2 system. The N_2 adsorption and XRD results indicate that the mesoporous Si-MCM-41 structure is well maintained during the support of Pt to form supported Pt catalyst as well as after the reaction of the resulting catalyst in NO–C_3H_6–O_2 system.

Figure 2 shows the XPS spectra of Pt_{4f} on 2% Pt/Si-MCM-41 before and after reaction in C_3H_6–NO–O_2 system, or after it has been reduced in H_2 at 500 °C for 1 h. The fresh sample of 2% Pt/Si-MCM-41 shows a broad binding energy peak from 72 to 78 eV, with Pt^{2+}, which has the pair binding

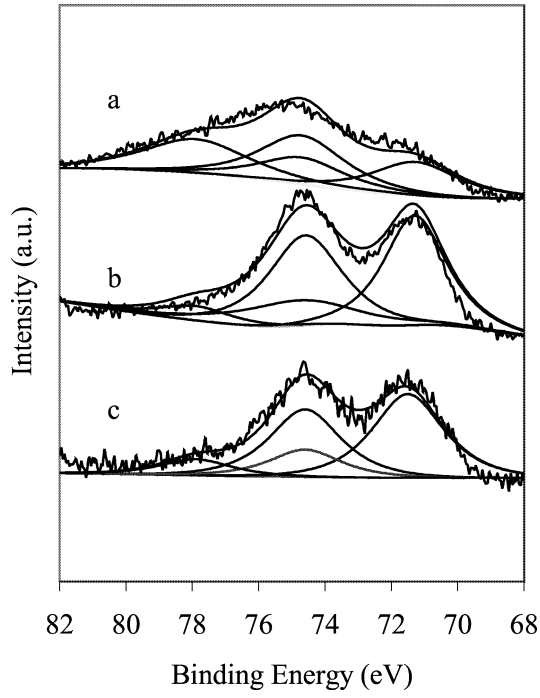

Fig. 2. Pt_{4f} XPS spectra of 2% Pt/Si-MCM-41 for (a) fresh sample, (b) after reaction in $C_3H_6 + NO + O_2$, (c) after reduction in H_2 at 500 °C for 1 h.

energy peaks at 74.6 and 77.9 eV [49], to be the majority species on the catalyst surface. After the deNO_x reaction in the gas mixture of $C_3H_6 + NO + O_2$ at temperatures from 200 to 500 °C, the two main binding energy peaks shift to 71.2 and 74.6 eV, respectively, which are the typical binding energies for Pt^0. The oxidized Pt species with bonding energy of 74.6 and 77.9 eV, then becomes the minority Pt species on the Pt/Si-MCM-41 catalyst. The XPS spectrum of the used catalyst is quite similar to that of the sample that has been reduced in H_2 at 500 °C and the reduced Pt species is the majority species on Si-MCM-41, despite the difference that the reaction has been performed in the presence of excess oxygen. The result implies that Pt species have been reduced during the selective catalytic reduction of NO in the presence of excess oxygen, suggesting that the interaction of oxidised Pt species with C_3H_6 is the necessary step during the reaction for the reduction of Pt species. A redox mechanism proposed by Burch et al. [50] for SCR-NO over Pt/SiO_2 suggests that NO could be reduced by C_3H_6 over Pt oxide via a redox process. Based on this redox mechanism, the adsorption of propene on the catalyst surface initially reduced the active sites, which might be essentially composed of isolated metal particles. Subsequently, on these reduced active sites, NO reduction or decomposition was facile and the surface became oxidised and deactivated for NO reduction.

Figure 3 shows the XPS spectra of Pt_{4f} on Pt/Si-MCM-41 catalysts after they have been treated in C_3H_6 and $C_3H_6 + O_2$. After treatment in C_3H_6 at 300 °C, the oxidised Pt species have been reduced, as can be seen by a comparison of the XPS spectra with those of the reduced Pt species in Fig. 2. From Fig. 3, it can be found that the two spectra are quite similar to each other although the treatment conditions are different. After treatment in $C_3H_6 + O_2$ at 300 °C, the oxidised Pt species are found to be still in the reduced state. The result implies that the adsorption of C_3H_6 is stronger than the adsorption of O_2 on the surface of Pt species. Even in the presence of a high concentration of O_2, the interaction of C_3H_6 with Pt species could not be affected.

The coupling reaction of the activation of hydrocarbon and the reduction of Pt species is suggested to be a significant step for the selective catalytic reduction of NO over Pt/Si-MCM-41 catalyst by hydrocarbon in the presence of excess oxygen. The reaction temperature for selective catalytic reduction of NO in the presence of excess oxygen is influenced by the reducible temperature of oxidised Pt species. As shown in Fig. 4, the reaction temperature required for maximum NO conversion on 1wt.% Pt/Si-MCM-41 catalyst is much lower than that on 1wt.% Pt/Al_2O_3 under the same reaction conditions. For 1wt.% Pt/Si-MCM-41, NO conversion increases sharply with temperature and reaches the maximum at 225 °C. For a comparison, NO conversion reaches the maximum at 270 °C over 1wt.% Pt/Al_2O_3 catalyst.

The reaction temperature for selective catalytic reduction of NO is found to be closely correlated with the reduction temperature of oxidised Pt species. The H_2-TPR profiles of 1wt.% Pt/Si-MCM-41 and 1wt.% Pt/Al_2O_3 are shown in Fig. 5. Most of the oxidised Pt species on the surface of Si-MCM-41 were found to be reduced by H_2 at lower temperatures at around 90–150 °C. For a comparison, the reduction temperature for Pt/Al_2O_3 is about 100 °C higher than that of Pt/Si-MCM-41. The higher activity of Pt/Si-MCM-41 than Pt/Al_2O_3 at lower temperature is suggested to be contributed by the lower reducible temperature of Pt species on Si-MCM-41 due to the better dispersion of Pt species on the high-surface-area Si-MCM-41 mesoporous material [39,51]. In addition, Burch et al. [38] found that Pt/SiO_2 also showed higher activity than Pt/Al_2O_3 and this is generally attributed to weaker metal-support interaction with the SiO_2. Since the framework wall of Si-MCM-41 is consisted of amorphous SiO_2, the interaction between Pt species and Si-MCM-41 may also be weaker than that with Al_2O_3. Thus the Pt species over Pt/Si-MCM-41 is easier to

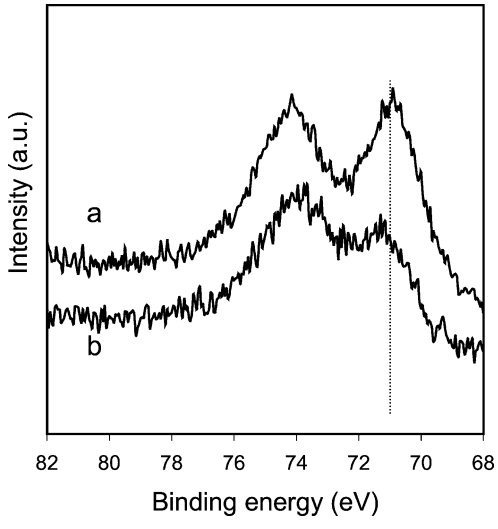

Fig. 3. Pt_{4f} XPS spectra of 2% Pt/Si-MCM-41 after treatment at 300 °C in (a) 1000 ppm of C_3H_6/He and (b) 1000 ppm of $C_3H_6 + 5$ vol.% of O_2.

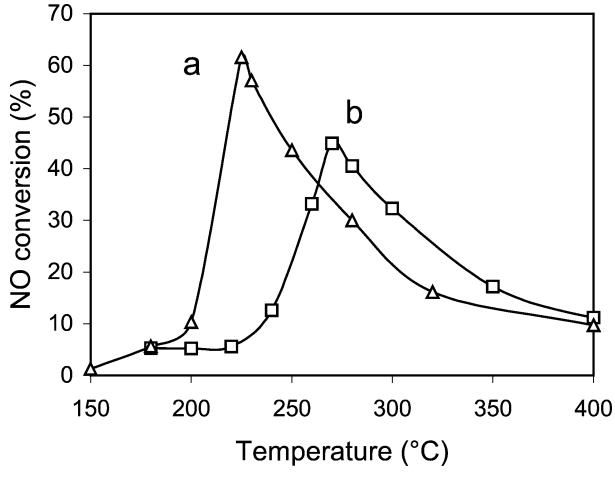

Fig. 4. NO conversion on (a) 1wt.% Pt/Si-MCM-41 and (b) 1wt.% Pt/Al_2O_3.

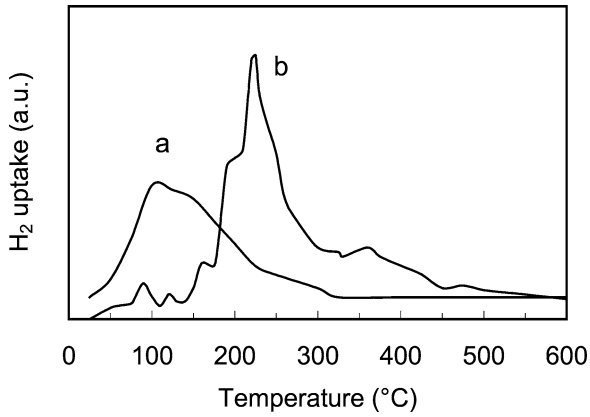

Fig. 5. H_2-TPR profiles of (a) 1wt.% Pt/Si-MCM-41 and (b) 1wt.% Pt/Al_2O_3.

be reduced at low temperature, resulting in its better activity at lower reaction temperature than Pt/Al_2O_3.

The redox mechanism [50] has suggested that the reduced Pt could be re-oxidised by the interaction of Pt with NO and O_2. However, Fig. 6 shows the Pt_{4f} XPS patterns of Pt/Si-MCM-41 after in contact with $C_3H_6 + O_2$ and followed by treatment in $O_2 + NO$. Although the oxidised Pt species could be reduced by C_3H_6 in the presence of O_2, however its binding energy is not obviously shifted to higher values following its treatment in pure oxidising environment of $NO + O_2$. The result implies that the reduced Pt is quite stable and not easy to be completely oxidised to the initial oxidation state by merely in contact with $O_2 + NO$ at the reaction temperature. Using in-situ XANES, Schießer found that the oxidation state of Pt species over Pt/Si-MCM-41 depended on the reaction temperature during the reaction of $NO–C_3H_6–O_2$ [47], where Pt species was reduced at low reaction temperature and oxidized at high reaction temperature. The treatment temperature in our study may be not high enough to oxidize the reduced Pt species. In addition, the ex-situ XPS measurement of our study may not reflect the real oxidation state of Pt species during the reaction as the oxidation state of Pt may be changed during the cooling stage of the treatment of the sample in the oxidizing gas mixture. The reduced Pt species is observed to be only partially oxidized by contacting with $O_2 + NO$ in our XPS study.

The oxidised Pt species was firstly reduced by C_3H_6 even in the presence of excess oxygen due to the strong adsorption and reaction between Pt and C_3H_6 at the reaction temperature. Meanwhile, C_3H_6 was oxidised on the active sites, forming intermediates ($C_xH_yO_z$ and CO) that may be associated with active Pt sites and react with NO. During the reduction of NO to N_2 and N_2O, the reduced Pt sites may be only partially oxidised, leaving O-species to be associated on the active sites. The adsorbed oxygen then interact with C_3H_6, consequently restoring the states of Pt sites to the reduced Pt^0 state and completing the catalytic cycle.

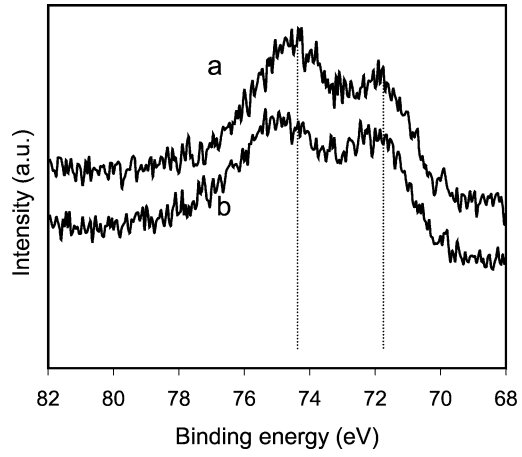

Fig. 6. Pt_{4f} XPS patterns of Pt/Si-MCM-41 catalyst (a) treated in $C_3H_6 + O_2$ at 300 °C for 1 h first and (b) then treated in $O_2 + NO$ at 300 °C for 1 h.

3.2. In-situ FTIR study

The reaction mechanism for the selective catalytic reduction of NO in the presence of excess oxygen over Pt-based catalyst was further studied by in-situ FTIR. Figure 7 shows the FTIR spectra of Pt supported on different catalysts after exposure to 1000 ppm NO + 1000 ppm C_3H_6 + 5% O_2 at 200 °C for 30 min. Strong absorbance peaks at 1585, 1464, 1394, and 1308 cm^{-1} are observed on Pt/Al_2O_3. These peaks can be assigned to the adsorbed carboxylates ($–COO^-$), in agreement with those reported in the literature

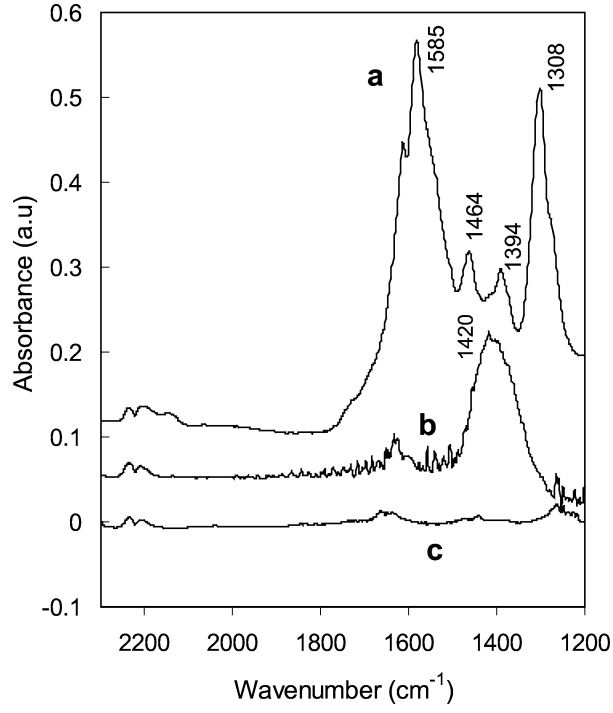

Fig. 7. In-situ infrared spectra at 200 °C of (a) 1wt.% Pt/Al_2O_3, (b) 1wt.% Pt/SiO_2, and (c) 1wt.% Pt/Si-MCM-41 after being exposed to 1000 ppm of NO + 1000 ppm of C_3H_6 + 5% of O_2 for 30 min.

[52,53]. IR peaks at 1585 and 1394 cm^{-1} can be assigned to adsorbed formate ions on alumina and are attributed to the asymmetric stretching vibration and the –CH bending vibration, respectively. The peak at 1464 cm^{-1} can be assigned to the vibration of an adsorbed acetate species, in agreement with literature. The IR absorbance peak at 1308 cm^{-1} can be assigned to the out of plane bending –CH of the surface acetates. The surface species of carboxylates adsorbed on Pt/Al_2O_3 was reported to be stable after being exposed to NO/O_2 at 250 °C, suggesting that they did not participate in the selective catalytic reduction of NO [54]. Most of these carboxylates species are suggested to be associated with Al_2O_3 support but not with active Pt sites as the spectra of Al_2O_3 are quite similar to those of Pt/Al_2O_3 catalyst. However, only one broad peak at 1420 cm^{-1} was observed on Pt/SiO_2 due to the absorbance of the reaction intermediates associated with SiO_2.

For a comparison, the intensity of the infrared absorbance of these reaction intermediates on Pt/Si-MCM-41 is much weaker than that of Pt/Al_2O_3 and Pt/SiO_2. The result indicates that the surface reaction is obviously affected by the different type of catalyst supports used in this study as the Pt loading is the same for all these different samples. Although the surface chemical property of SiO_2 and Si-MCM-41 is quite similar, the surface concentration of reaction intermediates on SiO_2 is much higher than that on Si-MCM-41. Based on the overall series reaction of

$$\mathrm{R} \xrightarrow{r_1} \mathrm{I} \xrightarrow{r_2} \mathrm{P} \qquad \text{(R1)}$$

where r_1 and r_2 are the reaction rate for each step and the symbols R, I, and P stand for reactants, intermediates, and products, respectively, the concentration of intermediates depends on the ratio of r_2/r_1. The FTIR results indicate that the surface concentration of intermediates on Pt/Si-MCM-41 is the lowest, indicating that the ratio of r_2/r_1 for Pt/Si-MCM-41 may be larger than that of Pt supported on Al_2O_3 and SiO_2. The results imply that the mesoporous Si-MCM-41 support facilitates the surface reaction between reaction intermediates and NO_x to form N_2 (or N_2O) or the decomposition of adsorbed reaction intermediates, resulting in the low surface concentration of these reaction intermediates adsorbed on Pt/Si-MCM-41. Similarly, it has been reported that different supports play an important role in the reaction mechanism of selective reduction of NO through the hydrocarbon activation [55].

Figure 8 shows the in-situ FTIR spectra of Pt/Si-MCM-41 recorded under various conditions at 200 °C for 30 min. After exposure to $NO + O_2 + C_3H_6$ or C_3H_6, a peak at 2065 cm^{-1} is observed. IR peak in this region is assigned to CO species adsorbed on Pt species [56]. CO bonded to a reduced metal atom is usually attached more strongly than CO bonded to the oxidized metal [57]. The surface CO species result from the partial oxidation of C_3H_6 on the catalyst surface. A set of peaks in the 1400–1700 cm^{-1} region (as observed in Figs. 8a and 8d) is due to the bending

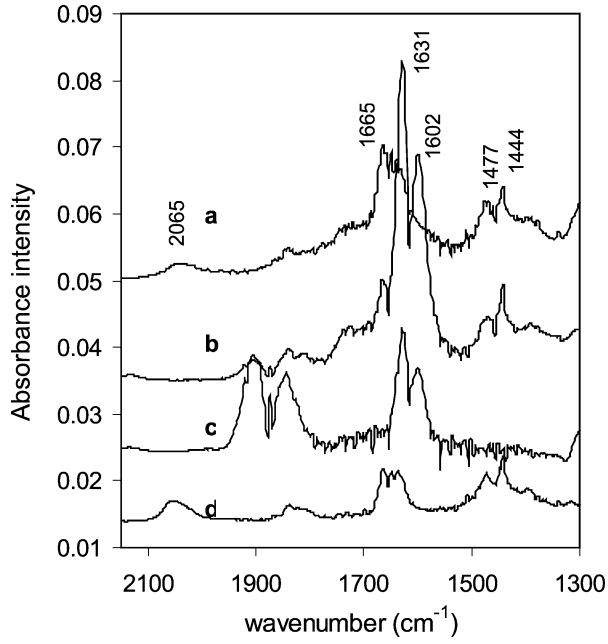

Fig. 8. FTIR spectra at 200 °C of Pt/Si-MCM-41 after 30-min exposure to (a) 1000 ppm of NO + 1000 ppm of C_3H_6 + 5% of O_2; (b) 1000 ppm of NO + 1000 ppm of C_3H_6; (c) 1000 ppm of NO; (d) 1000 ppm of C_3H_6.

vibration of the gas phase propylene and the partial oxidation intermediate adsorbed on the catalyst surface.

Figure 8c shows the spectrum of Pt/Si-MCM-41 after being exposed to 1000 ppm of NO in He at 200 °C. The doublet peaks at 1906 and 1851 cm^{-1} are attributed to the gas phase NO. The IR peaks in the range of 1600–1700 cm^{-1} characterise the formation of adsorbed surface species. Two peaks at 1631 and 1602 cm^{-1} can be assigned to nitrates (NO_3^-) adsorbed on the surface of Si-MCM-41. The nitrosium ion (–NO^-) linearly adsorbed on Pt, which should have a peak at 1740 cm^{-1}, is not clearly shown. It is suggested that the adsorbed NO may have interacted with surface O species to form NO_3^- and adsorbed on the surface of catalyst.

Figure 8d shows that exposure of the catalyst to C_3H_6 yields a higher absorbance intensity for CO species than exposure of the catalyst to $NO + O_2 + C_3H_6$. The reason may be explained as follows. The surface of Pt/Si-MCM-41 is saturated with adsorbed oxygen species during the pre-treatment in the O_2/He stream. As C_3H_6 may then be easily activated by surface oxygen to form CO species, more CO species are available to be adsorbed on the catalyst surface. Since surface platinum species are known to be easily reduced under flowing propylene and the reduced platinum species can strongly adsorb CO species, thus more CO species are adsorbed on the reduced platinum active sites.

When the catalyst is exposed to the reaction gas mixture containing no oxygen, some differences can be observed. For example, Fig. 8b shows the IR peak at 2065 cm^{-1} is not observed after exposure of the catalyst to $NO + C_3H_6$ at 200 °C. In addition to the gas phase C_3H_6 (in the range of

1400–1700 cm^{-1}), the IR peak for adsorbed NO_3^- is clearly shown. NO molecules compete with surface oxygen species for the interaction and occupation of the adsorption sites. After exposure of the catalyst under flowing NO + C_3H_6 for 30 min, no CO species was detected by FTIR due to the lack of surface oxygen species. C_3H_6 is difficult to be activated by merely having interaction with NO in the absence of surface oxygen species, leading to the inactivity of Pt/Si-MCM-41 for reduction of NO with C_3H_6 below 250 °C without oxygen in the reaction stream [39].

Figure 9 shows the spectra of the Pt/Si-MCM41 collected after exposure of the catalyst to the reaction gas mixture of NO + C_3H_6 + O_2 followed by flushing of the catalyst with 5vol.% O_2/He. During the first 5 min of the flushing of the catalyst with flowing oxygen, the intensities of IR peaks at the range of 1400–1700 cm^{-1} decrease quickly due to the removal of the gas phase hydrocarbon, leaving only surface adsorbed species on the catalyst surface. The intensity of CO peak becomes slightly weaker in 1 min, but it decreases significantly in 5 min and diminishes completely in 10 min. The result implies that CO species are not as stable as $-COO^-$ species adsorbed on Pt-based catalyst [54]. This may be attributed to the fact that the surface CO species participate in the catalytic reduction of NO.

After exposure of Pt/Si-MCM-41 to the reaction gas mixture for 1 h, the catalyst sample was flushed with 1000 ppm of C_3H_6 and the corresponding infrared spectra were taken under different flushing period. Fig. 10 shows the in-situ IR spectra characterizing the resulting surface species formed under different flushing period. It is found that the absorbance intensity of CO species on the catalyst surface increases with flushing time due to the strong interaction and reaction of C_3H_6 with surface oxygen species adsorbed on Pt.

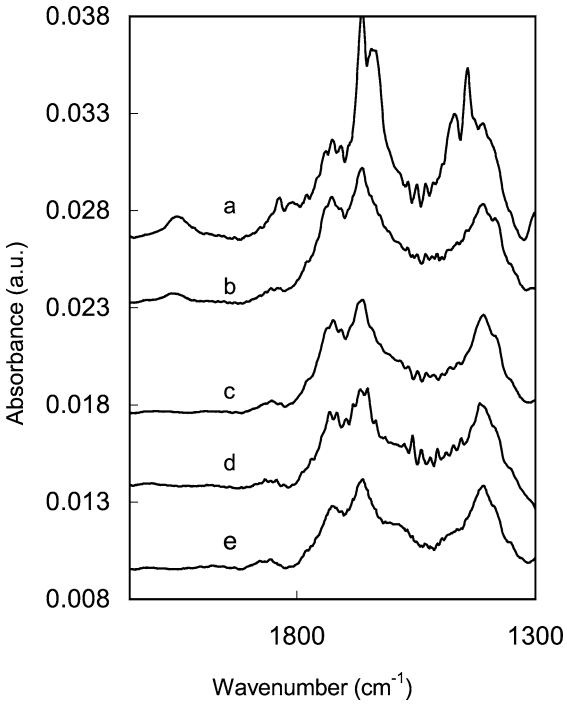

Fig. 9. In-situ IR spectra of Pt/Si-MCM-41 at 200 °C for (a) exposure to 1000 ppm NO + 1000 ppm C_3H_6 + 5% O_2 for 1 h; followed by flushing of (a) with 5% of O_2 in He for (b) 1 min, (c) 5 min, (d) 10 min, (e) 30 min.

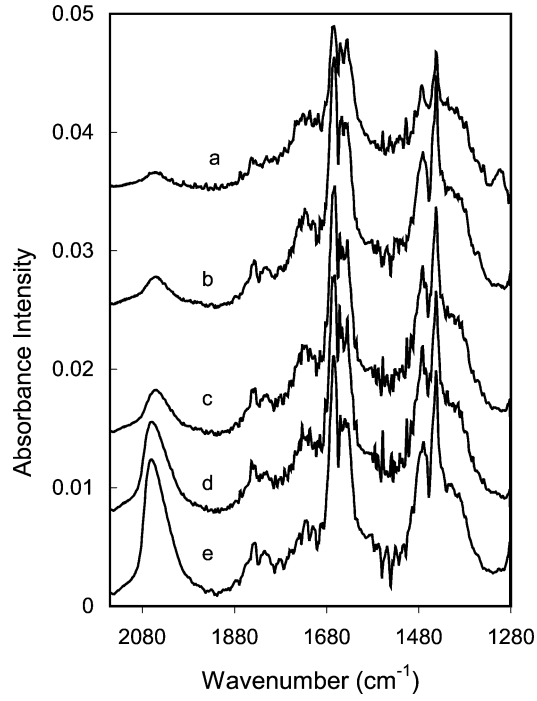

Fig. 10. In-situ IR spectra of Pt/Si-MCM-41 at 200 °C after (a) exposure to 1000 ppm of NO + 1000 ppm of C_3H_6 + 5% of O_2 for 1 h, followed by flushing of (a) with 1000 ppm of C_3H_6 (b) for 5 min; (c) for 10 min; (d) for 30 min; and (e) for 60 min.

The reactivity of surface CO species with NO was then investigated. Figure 11 shows in-situ FTIR spectra of Pt/Si-MCM-41 under treatment with flowing 2000 ppm of CO at 200 °C, followed by flushing of the sample with 2500 ppm

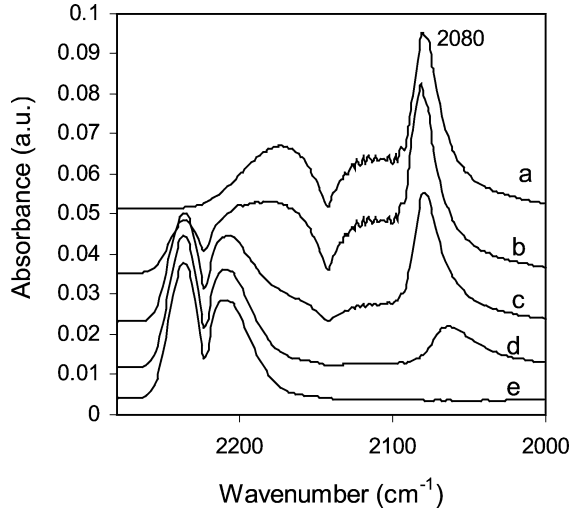

Fig. 11. In-situ FTIR spectra of (a) 1% Pt/Si-MCM-41 under treatment with flowing 2000 ppm of CO at 200 °C for 30 min, followed by flushing of (a) with 2500 ppm of NO at 200 °C for (b) 1 min, (c) 5 min, (d) 10 min, and (e) 15 min.

of NO for different periods. A strong peak is observed at 2080 cm^{-1}, which has been assigned to –CO linearly bonded to the reduced Pt atom. A broad low-intensity peak is also observed in the range of 2120–2180 cm^{-1}, which has been assigned to –CO species bonded to Pt oxide species. The peak intensity of linearly bonded CO species on the reduced Pt atoms decreases gradually during the first 5 min of flushing of the sample with 2500 ppm of NO. However, under the same treatment condition, the peak intensity of CO species adsorbed on Pt oxide species decreases quickly; this is due to the fact that the strength of adsorption of CO on Pt oxide species is much weaker than those on reduced Pt sites. After flushing of the CO-treated sample with NO for 10 min, the linearly bonded CO peak decreases significantly and shifts to 2067 cm^{-1}. Interestingly, this result is consistent with those observed with the flushing of the reaction mixture-treated sample with C_3H_6 (as shown in Fig. 10), confirming that CO is the reaction intermediate formed by the reaction of adsorbed propylene with surface oxygen species. A complete disappearance of the CO peak at 2069 cm^{-1} occurs after flushing of the CO-treated sample with NO for 15 min. Meanwhile, the doublet peaks at 2238 and 2215 cm^{-1} are attributed to the adsorbed NO species on the catalyst surface. It has been suggested that CO and NO should be adsorbed on the freely available Pt adsorption sites. Once NO dissociates, the two adsorbed N (i.e., N_{ad}) atoms adjacent to each other may combine to give N_2 and CO reacts with adsorbed O atoms to form CO_2. N_2 and CO_2 then desorb immediately, creating more free Pt adsorption sites available for NO dissociation. However, it should be noted that the actual reaction path may be more complicated than the above postulated reaction path. This is because the isolated N_{ad} may also react with NO_{ad} to form N_2O, which is one of main byproducts of the whole reaction. In addition, the isolated N_{ad} atoms may also be trapped by CO species to form NCO intermediate; this observation can be investigated by flushing the sample with CO to react CO with NO molecules pre-adsorbed on the catalyst surface.

Figure 12 shows the in-situ FTIR spectra of 1wt.% Pt/Si-MCM-41 under treatment in flowing NO at 200 °C, followed by flushing of the NO-treated sample first with He to remove the gas phase and physically adsorbed NO and then with 2000 ppm of CO in He to investigate the surface reaction between CO and the pre-adsorbed NO molecules on the catalyst surface. The doublet peaks at 2238 and 2215 cm^{-1} slightly decrease after flushing of the NO-treated sample with He for 5 min, indicating that NO is strongly adsorbed on the Pt sites. However, once the flush stream is switched to 2000 ppm of CO in He, the infrared bands characterizing the adsorbed NO molecules decrease rapidly in just 1 min. A new peak at 2177 cm^{-1} evolves after continuously flushing of the NO-treated sample in CO/He stream at 200 °C for 10 min. Since this band has been attributed to the asymmetric stretching of adsorbed NCO [58], the results imply that NCO may be one of the reaction intermediates formed during the selective catalytic reduction of NO by

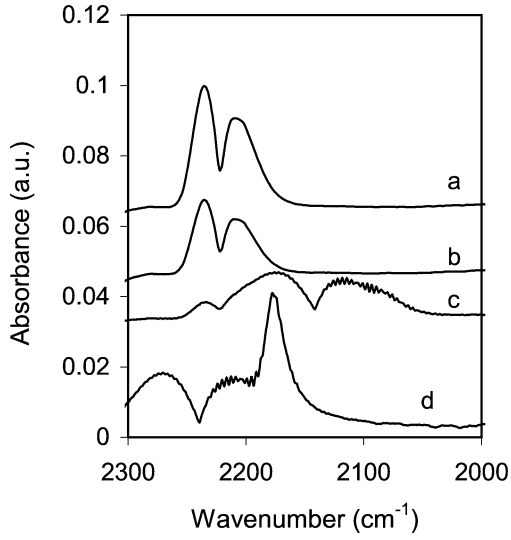

Fig. 12. In-situ FTIR spectra of (a) 1% Pt/Si-MCM-41 under treatment with flowing 2500 ppm of NO at 200 °C for 30 min; (b) flushing of (a) with He at 200 °C for 5 min; then followed by flushing of (b) with 2000 ppm of CO at 200 °C for (c) 1 min and (d) 10 min.

hydrocarbon in the presence of oxygen because, from the investigation of FTIR spectra of Pt/Si-MCM-41, CO has been shown to be formed from the reaction of hydrocarbon with surface oxygen species using reaction gas mixture.

Figure 13 shows the in-situ FTIR spectra of 1wt.% Pt/Si-MCM-41 under treatment with flowing 2500 ppm of NO at 200 °C for 1 h, followed by flushing of NO-treated sample with He first and then with reaction gas mixture consisting of 2000 ppm of C_3H_6 and 5% O_2 in He. The doublet infrared peaks (observed at 2237 and 2212 cm^{-1}) characterizing the pre-adsorbed NO species decrease faster in C_3H_6/O_2 stream than in pure He stream. The intensity of the peaks at 2237 and 2212 cm^{-1} decreases only slightly

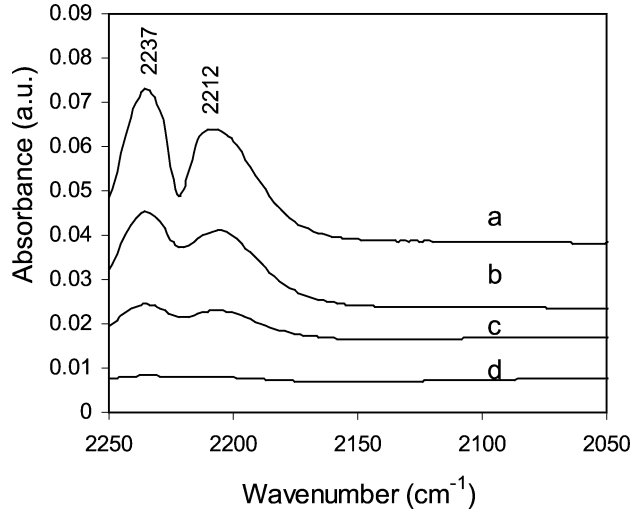

Fig. 13. In-situ FTIR spectra of (a) 1wt.% Pt/Si-MCM-41 under treatment with flowing 2500 ppm of NO at 200 °C for 1 h; (b) flushing of (a) with He at 200 °C for 10 min; followed by flushing of (b) with 2000 ppm of $C_3H_6 + 5\%\ O_2$ at 200 °C (c) for 10 min and (d) 20 min.

after flushing of the NO-treated sample with He for 10 min, but decreases significantly after flushing with C_3H_6/O_2 for the same period and diminished completely after 20 min. This result is quite similar to that obtained by flushing of the NO-treated sample with CO/He. This result indirectly confirms that CO, which could have been formed as the reaction intermediate from the reaction between C_3H_6 with surface oxygen species, might then react with NO to form N_2 or N_2O.

The exact reaction mechanism for the selective catalytic reduction of NO by C_3H_6 over Pt/Si-MCM-41 in the presence of excess oxygen is still not clear. However, based on the above results, we propose the following reaction mechanism:

$$C_3H_6(g) + * \rightarrow CH_n*, \quad \text{(R2)}$$

$$O_2(g) + * \rightarrow 2O*, \quad \text{(R3)}$$

$$NO(g) + * \rightarrow NO*, \quad \text{(R4)}$$

$$CH_n* + O* \rightarrow (C_xH_yO_z)* + CO* + CO_2 + H_2O, \quad \text{(R5)}$$

$$NO* + * \rightarrow N* + O*, \quad \text{(R6)}$$

$$NO* + CO* \rightarrow NCO* + O*, \quad \text{(R7)}$$

$$N* + CO* \rightarrow NCO*, \quad \text{(R8)}$$

$$NCO* + * \rightarrow N* + CO*, \quad \text{(R9)}$$

$$N* + N* \rightarrow N_2 + 2*, \quad \text{(R10)}$$

$$NO + N* \rightarrow N_2O + *, \quad \text{(R11)}$$

$$CO* + O* \rightarrow CO_2 + 2*, \quad \text{(R12)}$$

$$2NCO* \rightarrow N_2 + CO_2 + C* + *, \quad \text{(R13)}$$

$$C* + 2O* \rightarrow CO_2 + 3*. \quad \text{(R14)}$$

Three reactants (C_3H_6, NO, and O_2) are suggested to be adsorbed on the same type of Pt adsorption sites (denoted as $*$). Besides being completely oxidized, C_3H_6 can be dissociated to CH_n* on the catalyst surface and partially oxidised to $(C_xH_yO_z)$, such as formates and acetates or CO. The decomposition reaction path and the role of $(C_xH_yO_z)$ during the selective reduction of NO are still not clear. Carboxylate (–COO), which is one of the reaction intermediates, is believed not to participate in the HC-SCR reaction because it is found to be stubbornly adsorbed on the catalyst surface. However, CO, which is another reaction intermediate, is suggested to facilitate the selective reduction of NO on the catalyst surface. NO dissociates to $N*$ and $O*$ on the active Pt sites. N_2 may be formed from the combination of two adjacent $N*$, while N_2O from the adjacent $N*$ and NO. $NCO*$ may be formed from the interaction of $N*$ and $CO*$ or the surface reaction between $NO*$ and $CO*$. Two adjacent surface NCO species may decompose to N_2, CO_2 or surface carbonaceous species. The formation of surface carbonaceous species is not surprising as Pt catalyst has been found to be covered with carbonaceous species after exposing the catalyst to C_3H_6–NO–O_2 system; this has been attributed to the insufficient O species adsorbed on the catalyst surface to remove carbonaceous residues [50].

4. Conclusion

XPS results show that the oxidised Pt species over Si-MCM-41 could be reduced by hydrocarbon even in the presence of excess oxygen. Interestingly, the reduced Pt species could not be completely oxidised by NO/O_2 at the reaction temperature of 200–300 °C. The reduced Pt species act as free adsorbtion sites for NO, C_3H_6, and O_2 and as active sites for the dissociation of reactants and for the successive surface reactions. NO and O_2 may be dissociated to N and O atoms on the adsorption sites. After recombination of adsorbed N atoms adjacent to each other to form N_2 or interaction of adsorbed N atoms with adsorbed NO to form N_2O on the reduced sites, the residual O species adsorbed on the catalyst surface could not completely re-oxidize the Pt species.

CO is found to be a reaction intermediate playing a very important role for the selective catalytic reduction of NO by C_3H_6 in the presence of excess oxygen. Although carboxylates species are believed not to participate in the HC-SCR reaction, CO is suggested to facilitate the reduction of NO in this study. CO may react with NO to form NCO. The formation of these isocyanate species may then function as reaction pathways for the selective reduction of NO_x. However, the reaction mechanism for the whole deNO_x reaction is believed to be very complicated. The whole reaction network and main reaction pathways still remain unclear.

Acknowledgments

This work has been generously supported by the National Science and Technology Board of Singapore (R-297-000-093-303) and the National University of Singapore (R-297-000-093-112).

References

[1] M. Misono, Y. Hirao, C. Yokoyama, Catal. Today 38 (1997) 157.
[2] J.T. Miller, E. Glusker, R. Peddi, T. Zheng, J.R. Regalbuto, Catal. Lett. 51 (1998) 15.
[3] J.Y. Yan, H.H. Kung, W.M.H. Sachtler, M.C. Kung, J. Catal. 175 (1998) 294.
[4] K.A. Bethke, C. Li, M.C. Kung, B. Yang, H.H. Kung, Catal. Lett. 31 (1995) 287.
[5] T. Tanaka, T. Okuhara, M. Misono, Appl. Catal. B 4 (1994) L1.
[6] C. Yokoyama, M. Misono, J. Catal. 150 (1994) 9.
[7] L.J. Lobree, A.W. Aylor, A.J. Reimer, A.T. Bell, J. Catal. 169 (1997) 188.
[8] A.D. Cowan, N.W. Cant, B.S. Haynes, P.F. Nelson, J. Catal. 176 (1998) 329.
[9] N.W. Hayes, R.W. Joyner, E.S. Shpiro, Appl. Catal. B 8 (1996) 343.
[10] T. Beutel, B. Adelman, W.M.H. Sachtler, Catal. Lett. 37 (1996) 125.
[11] N.W. Hayes, W. Grünert, G.J. Hutchings, R.W. Joyner, E.S. Shpiro, J. Chem. Soc. Chem. Comm. 531 (1994).
[12] C. Li, K.A. Bethke, H.H. Kung, M.C. Kung, J. Chem. Soc. Chem. Comm. 813 (1995).

[13] S. Vergne, A. Berreghis, J. Tantet, C. Canaff, P. Magnoux, M. Guisnet, N. Davias, R. Noirot, Appl. Catal. B 18 (1998) 37.
[14] H. Takeda, M. Iwamoto, Catal. Lett. 38 (1996) 21.
[15] F. Poignant, J. Saussey, J.C. Lavalley, J.G. Mabilon, Catal. Today 29 (1996) 93.
[16] B.K. Cho, J.E. Yie, Appl. Catal. B 10 (1996) 263.
[17] M.D. Amiridis, T.J. Zhang, R.J. Farrauto, Appl. Catal. B 10 (1996) 203.
[18] M. Iwamoto, A.M. Hernandez, T. Zengyo, Chem. Commun. 37 (1997).
[19] K.L. Roberts, M.D. Amiridis, Ind. Eng. Chem. Res. 36 (1997) 3528.
[20] D.K. Captain, M.D. Amiridis, J. Catal. 184 (1999) 377.
[21] R. Burch, P.J. Millington, Catal. Today 29 (1996) 37.
[22] R. Burch, T.C. Watling, Stud. Surf. Sci. Catal. 116 (1998) 199.
[23] H. Hirabayashi, H. Yahiro, N. Mizuni, M. Iwamoto, Chem. Lett. 2235 (1992).
[24] H. Hamada, Y. Kintachi, M. Sasaki, T. Ito, M. Tabata, Appl. Catal. 75 (1991) L1.
[25] G.P. Ansell, S.E. Golunski, J.W. Hayes, A.P. Walker, R. Burch, P.J. Millington, Stud. Surf. Sci. Catal. 96 (1995) 577.
[26] R. Burch, Catal. Today 35 (1997) 27.
[27] P. Bourges, S. Lunati, G. Mabilon, Stud. Surf. Sci. Catal. 116 (1998) 213.
[28] M. Iwamoto, T. Zengyo, A.M. Hernandez, H. Araki, Appl. Catal. B 17 (1998) 259.
[29] R. Burch, P. Fornasiero, T.C. Watling, J. Catal. 176 (1998) 204.
[30] R. Burch, A.A. Shestov, J.A. Sullivan, J. Catal. 182 (1999) 497.
[31] B. Frank, G. Emig, A. Renken, Appl. Catal. B 19 (1998) 45.
[32] R. Burch, J.A. Sullivan, J. Catal. 182 (1999) 489.
[33] R. Burch, P. Fornasiero, B.W.L. Southward, J. Catal. 182 (1999) 234.
[34] K. Matsuoka, H. Orikasa, Y. Itoh, P. Chambrion, A. Tomita, Appl. Catal. B 26 (2000) 89.
[35] L. Olsson, H. Persson, E. Fridell, M. Skoglundh, B.J. Andersson, J. Phys. Chem. B 105 (2001) 6895.
[36] M. Sasaki, H. Hamada, Y. Kintachi, T. Ito, Catal. Lett. 15 (1992) 297.
[37] R. Burch, P.J. Millington, A.P. Walker, Appl. Catal. B 4 (1994) 65.
[38] R. Burch, P.J. Millington, Catal. Today 29 (1996) 37.
[39] R.Q. Long, R.T. Yang, Catal. Lett. 52 (1998) 91.
[40] W. Schießer, H. Vinek, A. Jentys, Catal. Lett. 56 (1998) 189.
[41] A. Jentys, W. Schießer, H. Vinek, Catal. Today 59 (2000) 313.
[42] A. Jentys, W. Schießer, H. Vinek, Stud. Surf. Sci. Catal. 125 (1999) 571.
[43] A. Jentys, W. Schießer, H. Vinek, Stud. Surf. Sci. Catal. B 130 (2000) 1523.
[44] S.C. Shen, S. Kawi, Catal. Today 68 (2001) 245.
[45] R.Q. Long, R.T. Yang, J. Phys. Chem. B 103 (1999) 2232.
[46] A. Jentys, W. Schießer, H. Vinek, Catal. Lett. 47 (1997) 193.
[47] W. Schießer, H. Vinek, A. Jnetys, Catal. Lett. 73 (2001) 67.
[48] W. Schießer, H. Vinek, A. Jnetys, Appl. Catal. B 33 (2001) 263.
[49] J.F. Moulder, W.F. Stickle, P.E. Sobol, K.D. Bomben, in: J. Chastain, E. Prairie (Eds.), Handbook of X-Ray Photoelectron Spectroscopy: A Reference Book of Standard Spectra for Identification and Interpretation of XPS data, Perkin–Elmer Corporation, Physical Electronics Division, 1992.
[50] R. Burch, T.C. Watling, Catal. Lett. 43 (1997) 19.
[51] N. Yao, C. Pinckney, S. Lim, C. Pak, G.L. Haller, Micropor. Mesopor. Mater. 44 (2000) 377.
[52] M. Xin, I.C. Hwang, S.I. Woo, J. Phys. Chem. B 101 (1997) 9005.
[53] G.R. Bamwenda, A. Ogata, A. Obuchi, J. Oi, K. Mizuno, J. Skrzypek, Appl. Catal. B 6 (1995) 311.
[54] D.K. Captain, M.D. Amiridis, J. Catal. 184 (1999) 377.
[55] J.M. Garcia-Cortes, J. Perez-Ramirez, M.J. Illan-Gomez, F. Kapteijn, J.A. Moulijn, Salinas-Martinez de Lecea, C. Appl. Catal. B 30 (2001) 399.
[56] M. Premet, J. Catal. 88 (1984) 273.
[57] T. Jin, Y. Zhou, G.J. Mains, J.M. White, J. Phys. Chem. 91 (1987) 5931.
[58] H. Miners, A.M. Bradshaw, P. Gardner, Phys. Chem. Chem. Phys. 1 (1999) 4909.